Chinese Chemical Letters 35 (2024) 109218

Contents lists available at ScienceDirect

Chinese Chemical Letters

journal homepage: www.elsevier.com/locate/cclet

Can perfluorooctanoic acid be effectively degraded using β-PbO_2 reactive electrochemical membrane?

Xubin Qian[a,b], Lei Xu[a,*], Xu Ge[a], Zhun Liu[c], Cheng Fang[d], Jianbing Wang[e], Junfeng Niu[a]

[a] College of Environmental Science and Engineering, North China Electric Power University, Beijing 102206, China
[b] College of Water Resources and Hydropower Engineering, North China Electric Power University, Beijing 102206, China
[c] Research Center for Eco-Environmental Engineering, Dongguan University of Technology, Dongguan 523808, China
[d] Global Centre for Environmental Remediation (GCER), University of Newcastle, Callaghan, NSW 2308, Australia
[e] School of Chemical and Environmental Engineering, China University of Mining and Technology (Beijing), Beijing 100083, China

ARTICLE INFO

Article history:
Received 8 June 2023
Revised 18 September 2023
Accepted 15 October 2023
Available online 17 October 2023

Keywords:
Perfluorooctanoic acid
β-PbO_2
Reactive electrochemical membrane
Electrochemical oxidation

ABSTRACT

Aqueous perfluorooctanoic acid (PFOA) elimination has raised significant concerns due to its persistence and bioaccumulation. Although β-PbO_2 plate anodes have shown efficient mineralization of PFOA, it remains unclear whether PFOA can be effectively degraded using β-PbO_2 reactive electrochemical membrane (REM). Herein, we assessed the performance of Ti/SnO_2-Sb/La-PbO_2 REM for PFOA removal and proposed a possible degradation mechanism. At a current density of 10 mA/cm^2 and a membrane flux of 8500 (liters per square meter per hour, LMH), the degradation efficiency of 10 mg/L PFOA was merely 8.8%, whereas the degradation efficiency of 0.1 mg/L PFOA increased to 96.6%. Although the porous structure of the β-PbO_2 REM provided numerous electroactive sites for PFOA, the generated oxygen bubbles in the pores could block the pore channels and adsorb PFOA molecules. These hindered the protonation process and significantly impeded the degradation of high-concentration PFOA. Quenching experiments indicated that $^{\bullet}$OH played dominant role in PFOA degradation. The electrical energy per order to remove 0.1 mg/L PFOA was merely 0.74 Wh/L, which was almost an order of magnitude lower than that of other anode materials. This study presents fresh opportunities for the electrochemical degradation of low-concentration PFOA using β-PbO_2 REM.

Perfluorooctanoic acid (PFOA), a forever chemical, has found extensive application in surfactants, lubricants and firefighting foams [1,2]. However, its persistence, bioaccumulation and potential hazards to human health have garnered global attention [3,4]. The accumulation of PFOA in the human body has been associated with various health risks, including cancer, liver damage, neurotoxicity, and endocrine disrupting [5–7]. To date, PFOA has been detected in various environment matrices such as water, sediment, breast milk and human blood [8]. Notably, in a public water system in New Jersey, PFOA was found at a concentration of 0.19 μg/L [9], while its concentration in groundwater at military bases reached 6.6 mg/L [10].

PFOA molecular has highly stable carbon-fluorine bonds (C-F, 116 kcal/mol) [11]. Natural decomposition, sand filtration and conventional microbiological degradation cannot efficiently remove PFOA from water [12]. Recently, various advanced treatment approaches have been investigated to eliminate PFOA from water, *e.g.*, ultrasonication [13], photocatalysis [14–16], zerovalent iron reduction [17], and microwave-hydrothermal [18], but they are usually limited by harsh reaction conditions and high energy consumption. Over the past decades, electrochemical oxidation process has been recognized as a promising technology for wastewater treatment due to its strong oxidation property, mild condition, and amenability to automation [19–22]. Electrochemical oxidation process can effectively destroy PFOA by direct electron transfer and $^{\bullet}$OH-mediated indirect oxidation process [23]. To data, born-doped diamond (BDD), Ti_4O_7 and β-PbO_2 anodes have been applied for the decomposition of PFOA [24–26]. For example, the degradation efficiency and first-order rate constant for 100 mg/L PFOA over 90 min were measured at 96.7% and 0.0370 min^{-1}, respectively, using a Ti/SnO_2-Sb/Ce-PbO_2 plate anode [27].

Reactive electrochemical membrane (REM) has been widely applied in the electrochemical oxidation of organic contaminants [28,29]. Compared to traditional plate anode, REM offers superior degradation performance attributed to its high active area and enhanced mass transfer rate, which effectively suppresses the diffusion boundary layer [30]. It was reported that 10 mg/L

* Corresponding author.
E-mail address: xulei@ncepu.edu.cn (L. Xu).

https://doi.org/10.1016/j.cclet.2023.109218
1001-8417/

carbamazepine was completely removed on TiO_2 nanotube arrays REM after 20 min degradation at 2 mA/cm^2, and the first-order degradation kinetic constant on flow-through mode (0.345 min^{-1}) was 38.3 times higher than that on flow-by mode (0.090 min^{-1}) [31]. In addition, previous studies have substantiated the exceptional electrochemical degradation performance of Ti_4O_7 REM when it comes to PFOA. For instance, the degradation efficiency of 2 μmol/L PFOA reached 73.9% on Magnéli phase Ti_4O_7 REM after 180 min at 8 mA/cm^2 [32]. Additionally, in a single pass-through mode at 3.3 V *vs.* SHE, with a hydraulic residence time of 11.3 s, the removal efficiency of 10 μmol/L PFOA on Ti_4O_7 REM exceeded 99.9% [33]. However, there still be a lack of studies on the electrochemical degradation of PFOA using β-PbO_2 REM, despite β-PbO_2 has been proved as an efficient plate anode in PFOA degradation. The degradation mechanism of PFOA on β-PbO_2 REM is still unclear, and it remains a question that whether PFOA can be effectively degraded on β-PbO_2 REM with enhanced mass transfer rate or not.

In this work, the electrochemical degradation of PFOA on Ti/SnO_2-Sb/La-PbO_2 REM (β-PbO_2 REM) was studied. The degradation performance of PFOA were compared at high and low concentration, and they were also investigated as functions of applied current densities and membrane fluxes. The electrochemical degradation mechanism of PFOA using β-PbO_2 REM was analyzed to provide basic data and theoretical support for the feasibility of PFOA removal on β-PbO_2 REM.

A complete list of materials is included in Text S1 (Supporting information). All solutions were prepared to use ultrapure water (from Milli-Q system) with a resistivity of 18.2 MΩ cm. Experiments were carried out in a flow-through electrochemical reactor, including a β-PbO_2 REM as working electrode and a porous titanium plate as counter electrode. The distance between the electrodes was 15 mm. The detailed preparation processes of β-PbO_2 REM were described in our previous work [25,29]. The total volume of solution was 300 mL with 25 mmol/L Na_2SO_4 as supporting electrolyte. The influencing factors such as applied current densities (5–20 mA/cm^2), PFOA initial concentrations (0.1–10.0 mg/L) and membrane fluxes (0-17000 LMH) (liters per square meter per hour, LMH) on the degradation performance of PFOA were investigated. In quenching experiments, 50 mmol/L, 500 mmol/L or 1000 mmol/L *tert*–butyl alcohol (TBA) was added as scavenger of $^{\bullet}$OH during the electrochemical degradation of PFOA. PFOA and short-chain perfluoroalkyl carboxylic acids (PFCAs) were analyzed by UPLC-MS/MS (Acquity UPLC H-Class/XEVO TQD, Waters), and the detail analytical methods are shown in Text S2 (Supporting information). The calculation method of the electrical energy per order (E_{EO}) and the observed oxidation kinetic rate constant (k_{obs}) for PFOA were described in Texts S3 and S4 (Supporting information), respectively.

Fig. 1a and Fig. S1a (Supporting information) illustrate the electrochemical oxidation performance of PFOA at different initial concentration, with a membrane flux of 8500 LMH and an applied current density of 10 mA/cm^2. The highest degradation efficiency and pseudo-first-order degradation kinetic constant (k) of PFOA were achieved at 0.1 mg/L, reaching 96.6% and 0.0344 min^{-1}, respectively (Table S1 in Supporting information). The degradation performance of PFOA showed a sharp decrease with its initial concentration increase. When the initial concentration increased from 0.1 mg/L to 10 mg/L, the corresponding k value decreased by 97.4%. Compared to the electrochemical degradation of PFOA in previous studies, β-PbO_2 REM demonstrates remarkable degradation performance for low-concentration PFOA (in the experimental concentration range). In contrast, the degradation performance of high-concentration PFOA using β-PbO_2 REM was the worst in the reported range (Table S2 in Supporting information). The k_{obs} value of 10 mg/L PFOA degradation (2.40×10^{-6} m/s) in this study was almost two orders of magnitude lower than that in previously reported result with Ti_4O_7 REM (1.30×10^{-4} m/s) [33]. During the electrolysis process, the β-PbO_2 anode exhibits a lower oxygen evolution potential (1.7–2.0 V *vs.* SHE) compared to the Ti_4O_7 anode (2.2–2.7 V *vs.* SHE) [30,34–36]. As a result, the β-PbO_2 anode is more prone to undergo the oxygen evolution reaction. Hence, there was a speculation that the formation of oxygen bubbles within the electroactive pores of β-PbO_2 REM could significantly impede the degradation process of high-concentration PFOA. Reaction sites and pore channels within the REM pore structure could be occupied by oxygen bubbles, and PFOA molecules could be adsorbed on the oxygen bubbles [19,37]. The protonation process, rate-limiting step of PFOA degradation, could not happen for the adsorbed PFOA molecules due to its non-direct contact with anode surface [23], resulting in the poor degradation performance of high-concentration PFOA using β-PbO_2 REM. Significantly, the removal amount of PFOA exhibited a notable decrease as the initial concentration increased from 5 mg/L to 10 mg/L. This could be attributed not only to the presence of oxygen bubbles but also to the heightened competition between the produced short-chain PFCAs and PFOA molecules for reaction sites and $^{\bullet}$OH. The above results illustrated that β-PbO_2 REM is an efficient anode in degradation of low-concentration PFOA. To further investigate the degradation mechanism of PFOA using β-PbO_2 REM, 0.1 mg/L PFOA was applied in the following experiments.

The effect of the membrane fluxes on PFOA degradation using β-PbO_2 REM at 10 mA/cm^2 is shown in Fig. 1b and Fig. S1b (Supporting information). The highest degradation efficiency (97.5%) and the k_{obs} value (9.47×10^{-5} m/s) were found at 17,000 LMH (Table S1 in Supporting information). The k_{obs} value was 4.2-fold higher than the reported result with porous Ti_4O_7 ceramic anode (2.27×10^{-5} m/s), with the reaction time of 90 min in our study and 180 min in the previous work [35]. When the membrane flux increased from 0 LMH (k_{obs} of 1.63×10^{-5} m/s) to 17000 LMH (k_{obs} of 9.47×10^{-5} m/s), the k_{obs} value increased by 5.3-fold. These significant improvements in degradation performance can be attributed to the higher mass transfer rate of PFOA molecules at higher membrane flux [30,38,39], as well as the more efficient utilization of REM pores at higher membrane flux, providing a larger electroactive area for PFOA degradation [40–42]. When the membrane flux increased from 4250 LMH to 17,000 LMH, the k_{obs} value exhibited a slow increase trend, which was similar to previous studies [29,43]. This was mainly because that the mass transfer performance tended to stabilize at high membrane flux, and the degradation process of PFOA became to be controlled by kinetic limitation [41,43]. Membrane flux increase could efficiently reduce the energy consumption for PFOA degradation (the embedded image in Fig. 1b). However, when the membrane flux increased from 8500 LMH to 17,000 LMH, the E_{EO} value decreased by 0.05 Wh/L showing a relatively stable state. That was mainly because of the following two reasons: (1) The electrochemical degradation process was almost controlled by the kinetic limit at the higher membrane flux, resulting in less variation in energy consumption [41].

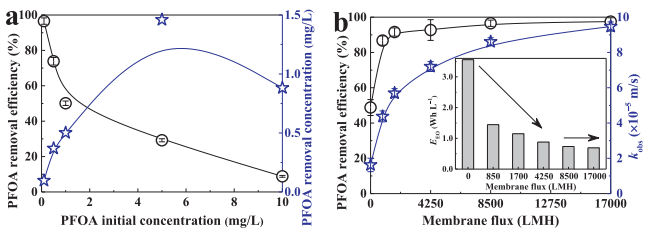

Fig. 1. Removal efficiency of PFOA at different experimental conditions: (a) initial concentration, and (b) membrane flux.

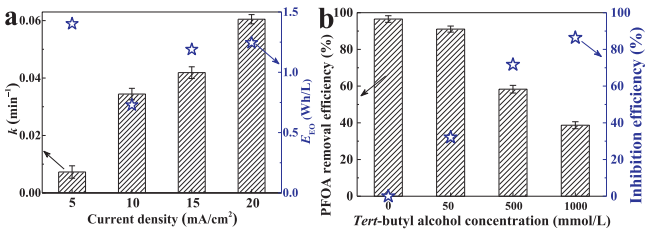

Fig. 2. Effects of (a) current density and (b) TBA concentration on the degradation of PFOA.

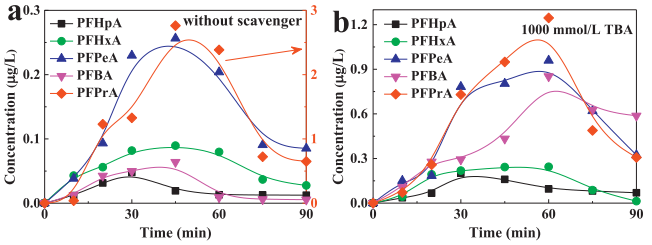

Fig. 3. The concentration of degradation intermediates of PFOA as a function of reaction time: (a) without scavenger and (b) in the presence of 1000 mmol/L TBA.

(2) The oxygen evolution and hydrogen evolution reactions at the electrode interface generate a significant number of small bubbles at higher membrane flux, thereby providing a larger specific surface area and more adsorption sites [44]. PFOA molecules might be easily adsorbed on these small bubbles, thus impeding the reduction of energy consumption.

Applied current density can greatly affect the electrochemical oxidation performance as shown in Fig. 2a and Fig. S1c (Supporting information). The k values of PFOA degradation exhibited a positively relationship with the applied current densities, which was similar to the previous studies [25,32]. The removal efficiency and k value of PFOA reached up to 99.2% and 0.0605 min^{-1}, respectively, at 20 mA/cm^2 (Table S1). The k value increased by almost an order of magnitude as the applied current density raised from 5 mA/cm^2 to 20 mA/cm^2. Higher current density means higher anode potential and stronger $^{\bullet}OH$ production capacity [45], which was conducive to improving the protonation process and degradation efficiency of PFOA at the anode. The calculated E_{EO} value increased from 0.74 Wh/L to 1.24 Wh/L when the applied current density increased from 10 mA/cm^2 to 20 mA/cm^2. There were more competing reactions, oxygen evolution reaction and hydrogen evolution reaction, generated at higher anode potential, resulting in energy waste. Notably, the maximum E_{EO} value (1.41 Wh/L) appeared at the lowest current density (5 mA/cm^2), which was caused by the lower degradation efficiency to significant increase the reaction time. Compared to other anode materials such as BDD, RuO_2, Ti_4O_7 and β-PbO_2 used for the electrochemical degradation of PFOA, the E_{EO} value obtained in this study (0.74 Wh/L) was nearly an order of magnitude lower than the lowest E_{EO} value (5.00 Wh/L) reported in the literatures (Table S3 in Supporting information). This indicates that β-PbO_2 REM is an energy-efficient and promising anode material for low-concentration PFOA degradation.

TBA was added as quenching agent during the electrochemical degradation to further evaluate the function of $^{\bullet}OH$ towards PFOA degradation. As shown in Fig. 2b, PFOA degradation was greatly retarded by TBA addition. The inhibition efficiencies were 32.1%, 71.5% and 86.3% at TBA concentration of 50 mmol/L, 500 mmol/L and 1000 mmol/L, respectively, according to the previous calculation method (Text S5 in Supporting information) [46]. It was proved that $^{\bullet}OH$ played a dominant role in PFOA degradation using advanced oxidation processes [47,48]. There was still a degradation efficiency of PFOA in the presence of 1000 mmol/L TBA, which could be the attribution of unquenched $^{\bullet}OH$ or even $SO_4^{\bullet-}$. $SO_4^{\bullet-}$ was proved as also an effective oxidation agent in PFOA degradation [49,50]. Sulfate in solution could be activated to $SO_4^{\bullet-}$ at anode surface, where is a strong acidic micro-environment during the electrochemical oxidation process ($SO_4^{2-} - e^- \rightarrow SO_4^{\bullet-}$) [51]. Therefore, PFOA might be degraded by $^{\bullet}OH$ and $SO_4^{\bullet-}$ after protonation process.

The degradation of short-chain PFCAs intermediates is more difficult than PFOA due to their weak reactivity and high hydrophily [52]. The degradation efficiencies of PFPeA (C5), PFBA (C4) and PFPrA (C3) on β-PbO_2 REM were all lower than 10% as shown in Fig. S2 (Supporting information). To further investigate the feasibility of degradation of low-concentration PFOA on β-PbO_2 REM, the concentrations of degradation intermediates in the aqueous solution were measured. As shown in Fig. 3a, the concentration of PFHpA (C7) peaked at 30 min (0.048 μg/L), and then decreased with reaction time. The concentrations of PFHxA (C6), PFPeA, PFBA and PFPrA declined after reaching their peaks at 45 min. This phenomenon suggested that PFOA can be degraded to short-chain PFCAs through a stepwise CF_2 flake-off manner during the electrochemical oxidation as proved in our previous study [23,27]. In addition, the accumulated low concentrations of all short-chain PFCAs indicated that they were effectively decomposed on the β-PbO_2 REM surface and merely few short-chain PFCAs released from anode surface into the bulk solution [53]. The relatively high concentration of PFPrA might be due to its strong hydrophilicity, resulting in weaker hydrophobic and van der Waals forces at the electrode interface, causing its highest concentration among the intermediates [54].

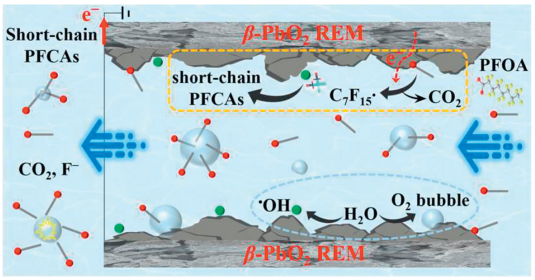

Fig. 4. Schematic diagram of degradation mechanism of PFOA on β-PbO_2 REM.

When 1000 mmol/L TBA was added in the electrochemical degradation of PFOA, the maximum concentrations of PFHpA, PFHxA, PFPeA, PFBA and PFPrA were measured at 0.202 μg/L, 0.244 μg/L, 0.959 μg/L, 0.852 μg/L and 1.245 μg/L, respectively (Fig. 3b). The detected concentrations of PFHpA, PFHxA, PFPeA and PFBA in the presence of 1000 mmol/L TBA were higher than those without scavenger. Meanwhile, the required reaction times to reach the maximum concentration of PFHxA, PFPeA, PFBA and PFPrA increased from 45 min to 60 min. These results suggested that TBA inhibited the degradation performance of the formed short-chain PFCAs intermediates on β-PbO_2 REM surface, leading to an increase in their concentration in the aqueous solution. Notably, the decreased concentration of PFPrA in the presence of TBA could be attributed to a significantly reduced decomposition performance of PFOA and also to the slower degradation of PFHpA, PFHxA, PFPeA, and PFBA, which further suggested that PFOA was decomposed through the stepwise CF_2 flake-off manner. The aforementioned results further indicated that $^{\bullet}OH$ played a vital and dominant role in the electrochemical degradation of the formed short-chain PFCAs.

Fig. 4 illustrates the possible degradation mechanism of PFOA on β-PbO_2 REM. Firstly, the PFOA molecules underwent a protonation process on the β-PbO_2 REM surface, and then were further

oxidized by $^{\bullet}OH$ and $SO_4^{\bullet-}$. Subsequently, the formed short-chain PFCAs were also efficiently degraded on the anode surface. However, the generated oxygen bubbles would adsorb PFOA molecules to hinder the protonation process, which severely limited the degradation efficiency of PFOA. The adsorbed PFOA molecules might be released into the solution as the bubbles burst and then be degraded. In contrast, Ti_4O_7 REM exhibited outstanding degradation performance for different concentration ranges of PFOA, mainly because of its high oxygen evolution potential, which could reduce the adverse effect of bubbles by controlling a low reaction potential.

In this study, β-PbO_2 REM showed remarkable degradation performance towards low-concentration PFOA, without abundant accumulation of short-chain PFCAs intermediates. The electrical energy per order to remove 0.1 mg/L PFOA was merely 0.74 Wh/L, which is notably lower than the values reported in the literatures. However, a crucial challenge for the efficient application of PFOA degradation using β-PbO_2 REM is how to eliminate oxygen bubbles within the REM pores during the degradation process. The collapse of bubbles and the mass transfer enhance of PFOA could be achieved with the assistance of ultrasound [19,55]. Additionally, the hydrophobic modification of the anode could enhance its hydrophobic affinity with PFOA and increase its oxygen evolution potential [34], thereby mitigating the adverse effects of the oxygen bubbles. To enhance the effectiveness of the PFOA treatment approach, it is essential to construct an ultrasound-assisted electrochemical oxidation system utilizing β-PbO_2 REM. Moreover, optimizing the hydrophobic modification of β-PbO_2 REM and thoroughly examining the operational performance of REMs in multiple series are crucial steps. These measures will significantly contribute to improving the feasibility of the PFOA treatment strategy.

Declaration of competing interest

The authors declare that they have no known competing financial interests or personal relationships that could have appeared to influence the work reported in this paper.

Acknowledgments

This study was financially supported by the National Key Research and Development Program (No. 2022YFE0135700), the National Natural Science Foundation of China (Nos. 52000028, 52370076 and 51978658), the Fundamental Research Funds for the Central Universities (No. 2023MS063), and Australian Research Council (No. G180200015).

Supplementary materials

Supplementary material associated with this article can be found, in the online version, at doi:10.1016/j.cclet.2023.109218.

References

[1] C. Liu, K.Y. Gin, V.W. Chang, B.P. Goh, M. Reinhard, Environ. Sci. Technol. 45 (2011) 9758–9764.
[2] C.A. Moody, J.A. Field, Environ. Sci. Technol. 34 (2000) 3864–3870.
[3] M. Houde, J.W. Martin, R.J. Letcher, K.R. Solomon, D.C. Muir, Environ. Sci. Technol. 40 (2006) 3463–3473.
[4] D. Ellis, J. Martin, S. Mabury, et al., Environ. Sci. Technol. 37 (2003) 3816–3820.
[5] V. Barry, A. Winquist, K. Steenland, Environ. Health Perspect. 121 (2013) 1313–1318.
[6] S.S. White, S.E. Fenton, E.P. Hines, J. Steroid Biochem. 127 (2011) 16–26.
[7] N. Onishchenko, C. Fischer, W.N.W. Ibrahim, et al., Neurotox. Res. 19 (2011) 452–461.
[8] Y.L. Mak, S. Taniyasu, L.W.Y. Yeung, et al., Environ. Sci. Technol. 43 (2009) 4824–4829.
[9] G.B. Post, J.B. Louis, K.R. Cooper, B.J. Boros-Russo, R.L. Lippincott, Environ. Sci. Technol. 43 (2009) 4547–4554.
[10] C.A. Moody, J.A. Field, Environ. Sci. Technol. 33 (1999) 2800–2806.
[11] B.D. Key, R.D. Howell, C.S. Criddle, Environ. Sci. Technol. 31 (1997) 2445–2454.
[12] S. Takagi, F. Adachi, K. Miyano, et al., Water Res. 45 (2011) 3925–3932.
[13] J. Lin, C. Hu, S. Lo, Ultrason. Sonochem. 28 (2016) 130–135.
[14] X. Li, P. Zhang, L. Jin, et al., Environ. Sci. Technol. 46 (2012) 5528–5534.
[15] X. Li, P. Zhang, L. Jin, et al., Chin. Chem. Lett. 30 (2019) 2225–2230.
[16] Y. Wang, P. Zhang, G. Pan, H. Chen, Chin. Chem. Lett. 19 (2008) 371–374.
[17] H. Hori, Y. Nagaoka, A. Yamamoto, et al., Environ. Sci. Technol. 40 (2006) 1049–1054.
[18] Y. Lee, S. Lo, P. Chiueh, D. Chang, Water Res. 43 (2009) 2811–2816.
[19] L. Xu, X. Qian, K. Wang, C. Fang, J. Niu, J. Clean. Prod. 263 (2020) 121546.
[20] D. Guo, S. You, F. Li, Y. Liu, Chin. Chem. Lett. 33 (2022) 1–10.
[21] L. Xu, X. Cui, J. Liao, et al., Chin. Chem. Lett. 33 (2022) 3701–3704.
[22] S. Tnag, Z. Luo, J. Liao, et al., Chin. Chem. Lett. 34 (2022) 108090.
[23] J. Niu, H. Lin, C. Gong, X. Sun, Environ. Sci. Technol. 47 (2013) 14341–14349.
[24] S. Liang, R.D. Pierce Jr, H. Lin, S.Y. Chiang, Q.J. Huang, Remediation 28 (2018) 127–134.
[25] H. Lin, J. Niu, S. Ding, L. Zhang, Water Res. 46 (2012) 2281–2289.
[26] F. Liu, S. Jiang, S. You, Y. Liu, Front. Environ. Sci. Eng. 17 (2023) 18.
[27] J. Niu, H. Lin, J. Xu, H. Wu, Y. Li, Environ. Sci. Technol. 46 (2012) 10191–10198.
[28] Y. Liu, F. Li, Q. Xia, et al., Nanoscale 10 (2018) 4771–4778.
[29] L. Xu, X. Ma, J. Niu, J. Chen, C. Zhou, J. Hazard. Mater. 379 (2019) 120692.
[30] C. Trellu, B.P. Chaplin, C. Coetsier, et al., Chemosphere 208 (2018) 159–175.
[31] L. Xu, J. Niu, H. Xie, et al., J. Hazard. Mater. 402 (2021) 123530.
[32] L. Yang, W. Yang, S. Lv, et al., Environ. Res. 204 (2022) 111995.
[33] T.X.H. Le, H. Haflich, A.D. Shah, B.P. Chaplin, Environ. Sci. Technol. Lett. 6 (2019) 504–510.
[34] X. Qian, K. Peng, L. Xu, et al., Chem. Eng. J. 429 (2022) 132309.
[35] H. Lin, J. Niu, S. Liang, et al., Chem. Eng. J. 354 (2018) 1058–1067.
[36] G. Chen, Sep. Purif. Technol. 38 (2004) 11–41.
[37] H. Liu, A. Vajpayee, C.D. Vecitis, ACS Appl. Mater. Interfaces 5 (2013) 10054–10066.
[38] A.M. Zaky, B.P. Chaplin, Environ. Sci. Technol. 47 (2013) 6554–6563.
[39] L. Jin, S. You, N. Ren, B. Din, Y. Liu, Environ. Sci. Technol. 56 (2022) 11750–11759.
[40] X. Qian, L. Xu, Y. Zhu, H. Yu, J. Niu, Chem. Eng. J. 420 (2021) 127615.
[41] L. Guo, Y. Jing, B.P. Chaplin, Environ. Sci. Technol. 50 (2016) 1428–1436.
[42] H. Liu, C.D. Vecitis, J. Phys. Chem. C 116 (2012) 374–383.
[43] K. Yang, H. Lin, S. Liang, et al., RSC Adv. 8 (2018) 13933–13944.
[44] Y. Li, G. Yang, S. Yu, et al., Int. J. Hydrog. Energy 44 (2019) 28283–28293.
[45] A. Urtiaga, C. Fernández-González, S. Gómez-Lavín, I. Ortiz, Chemosphere 129 (2015) 20–26.
[46] J. Cai, M. Zhou, Y. Pan, X. Du, X. Lu, Appl. Catal. B 257 (2019) 117902.
[47] Z. Zhang, J.J. Chen, X.J. Lyu, H. Yin, G.P. Sheng, Sci. Rep. 4 (2014) 1–6.
[48] S.M. Mitchell, M. Ahmad, A.L. Teel, R.J. Watts, Environ. Sci. Technol. Lett. 1 (2014) 117–121.
[49] Y. Yuan, L. Feng, X. He, et al., J. Hazard. Mater. 423 (2022) 127176.
[50] S. Sühnholz, A. Gawel, F.D. Kopinke, K. Mackenzie, Chem. Eng. J. 423 (2021) 130102.
[51] Y. Liu, X. Fan, X. Quan, et al., Environ. Sci. Technol. 53 (2019) 5195–5201.
[52] Y. Wang, H. Shi, C. Li, Q. Huang, Environ. Sci. Water Res. 6 (2020) 144–152.
[53] K. Wang, D. Huang, W. Wang, et al., Sci. Total Environ. 758 (2021) 143666.
[54] Y. Chen, M. Bhati, B.W. Walls, et al., Environ. Sci. Technol. 56 (2022) 8942–8952.
[55] X. Meng, Z. Liu, X. Qian, et al., J. Clean. Prod. 383 (2023) 135419.